JOURNAL OF SPACECRAFT AND ROCKETS
Vol. 40, No. 3, May–June 2003

Probabilistic Methods for Aerospace System Conceptual Design

Natasha Smith* and Sankaran Mahadevan†
Vanderbilt University, Nashville, Tennessee 37235

Two important objectives for the development of a second-generation reusable launch vehicle are concerned with significantly reducing cost and risk. Meeting these objectives requires a progressive design approach that eliminates noncompetitive designs as early in the process as possible. During these early stages, designs are usually evaluated at a low-fidelity conceptual level. Nevertheless, design decisions need to be made that significantly affect both cost and risk. Thus, it is crucial that both of these factors are considered during conceptual design. Methods to facilitate system risk assessment and risk vs cost allocation during the conceptual design of an aerospace system are presented. The analysis and optimization take into account the uncertainties in design variables that have important effects on safety, performance, and cost. The proposed methodology is illustrated for the geometry design of a reuseable launch vehicle.

Nomenclature

$a_{\rm bf}$ = body-flap area ratio, $\mathrm{ft}^2/\mathrm{ft}^2$
$a_{\rm tf}$ = tip-fin area ratio, $\mathrm{ft}^2/\mathrm{ft}^2$
a_w = wing area ratio, $\mathrm{ft}^2/\mathrm{ft}^2$
b_l = ballast weight fraction (lb/lb)
C_m = pitching moment coefficient
g = limit state function
P_f = probability of failure
r_f = fuselage finess ratio, ft/ft
r_m = mass ratio (lb/lb)
W = vehicle dry weight (lb)
X' = vector of reduced normal variables
X'^* = most probable point
α = direction cosine
β = reliability index
μ = mean value
σ = standard deviation
Φ = standard normal cumulative distribution function
∇ = gradient

Introduction

THE maturity of the aerospace industry is reflected in the modern challenge of engineering increasingly complex systems. At the same time, there exists a heightening priority to assess and design for cost effectiveness and reliability. As a result, design goals for future-generation systems are being expressed in terms of risk and cost. For example, goals for next generation reusable launch vehicles (RLV) include improving safety to achieve a less than 1/10,000 risk of crew loss and reducing cost to \$1000/lb or less for payload delivery.[1] These goals represent a tenfold improvement in cost and a one-hundredfold improvement in the reliability over the current space shuttle system. Whether they are achievable remains to be seen; first, multiple design approaches and several emerging technologies need to be evaluated and compared. Assessing risk and cost for these new systems with emerging technologies is extremely difficult. Historical databases based on legacy systems have questionable application to novel systems. Analytical models are an alternative, but have their own limitations. A traditional approach to design (in which disciplinary analysis is done independently and in sequence) would be extremely expensive and time consuming for this kind of comparative evaluation. Furthermore, risk design requirements given in probabilistic terms, that is, required probabilities of success or failure, cannot be targeted through conventional deterministic design methods (which deal with risk in terms of factors of safety). Thus, a design process that effectively balances cost and risk needs to incorporate multidisciplinary, concurrent design techniques along with probabilistic analysis in an optimization framework.

To meet the second-generation RLV goals, a multidisciplinary integration and optimization strategy is needed. In the early conceptual stage, designs need to be evaluated more quickly when less detail is available. At this stage, lower-fidelity models may be acceptable (assuming that these models do not sacrifice essential performance characteristics) because the desire is to identify the most attractive designs for further development. As designs are developed in more detail, that is, during preliminary and detailed design phases, higher-fidelity analysis tools can be employed. For example, response surface models for system performance are used during the early stages of conceptual design; they allow for quick analysis and easy optimization. Integration of higher-fidelity analysis codes across disciplines is more challenging, and so they are reserved for designs after further development. At the later stages, more expensive analysis through wind-tunnel experiments and component level tests are appropriate. In addition, the sensitivity of design elements to overall cost and risk influence the level of fidelity required at each stage of development.

Decisions that have the greatest effect on system risk and cost are made during the conceptual design stage. For this reason, despite the lower fidelity of the tools used, cost and risk evaluation and optimization needs to be a vital part of conceptual design analysis. It is also recognized that such design decisions need to account for the uncertainties in design variables that significantly impact cost and risk. However, current methods of system performance and risk assessment, capable of including uncertainty effects, are typically employed only after the system has been designed in detail and, in some cases, manufactured and tested. This stage is quite late in the system development process when it is difficult to make adjustments that would significantly reduce either cost or risk. Therefore, reliability analysis methods that can be applied during conceptual design and incorporated in a multidisciplinary system are needed.

To incorporate effectively probabilistic analysis in a progressive design strategy that builds from conceptual design (with low-fidelity models) to detailed design (with high-fidelity models), the following capabilities are needed during the early stages of design: 1) failure sequence diagram construction[2–4] without detailed information, based on initial concepts and approximate component descriptions; 2) probabilistic system reliability analysis[5–7]; 3) sensitivity analysis linkages between system events, component events, and major design variables[8,9]; 4) risk vs cost tradeoff computations at component

Received 13 May 2002; presented as Paper 2002-5583 at the AIAA/ISSMO 9th Symposium on Multidisciplinary Analysis and Optimization, Atlanta, GA, 4–6 September 2002; revision received 11 November 2002; accepted for publication 12 November 2002.

*Ph.D. Student, Civil and Environmental Engineering. Student Member AIAA.

†Professor, Civil and Environmental Engineering, Box 1831-B; sankaran.mahadevan@vanderbilt.edu. Senior Member AIAA.

and system levels[10,11]; and 5) risk allocation using a combination of optimization and Bayesian statistical analysis methods.[12–15] These capabilities are being developed for the second-generation RLV conceptual design at Vanderbilt University in collaboration with researchers at NASA Langley Research Center. In this paper, a deterministic optimization application for an RLV conceptual design originally developed by Unal et al.,[16] is modified for probabilistic system reliability analysis and optimization. This paper demonstrates capabilities 2 and 4 from the aforementioned set of needed probabilistic analysis tools. Furthermore, this application shows the significance of probabilistic effects at any stage of design.

The paper begins with a review of RLV design formulations given as multidisciplinary optimization problems and strategies that have been employed to solve them. Next, probabilistic analysis and optimization methods used in previous applications are discussed. These two concepts are synthesized by the application of probabilistic optimization to multidisciplinary RLV design. The following two sections explain the details of the deterministic problem and then describe its modification for probabilistic optimization. Finally, numerical results from the probabilistic optimization for the application example are computed and discussed.

Multidisciplinary Optimization in RLV Design

Design of the RLV is a complex process requiring analysis and optimization across multiple disciplines. In many cases, relatively mature (high- and low-fidelity) disciplinary analysis tools are available. These disciplinary analyses cannot be taken in isolation because they are coupled to one another through shared input and output. Furthermore, system design objectives and constraints may span several disciplines. Thus, a design process needs to address issues of the coupled multidisciplinary system. Integrating disciplinary analyses into a multidisciplinary framework and finding practical ways to solve system optimization problems is a serious challenge.

The first aspect of the multidisciplinary design challenge lies in building a system analysis from a collection of disciplinary analyses. The system architecture must be thoroughly understood to identify how the individual disciplines are coupled. In addition to this technical challenge, organizational and/or computational difficulties often present the largest obstacles in creating a multidisciplinary analysis. The second aspect of the challenge is in solving system optimization problems for the purpose of design. Here, the complexity, stability, and efficiency of the system analysis have significant consequences.

Several studies have addressed RLV design as a multidisciplinary optimization (MDO) problem[16–19] and developed strategies on a number of fronts. One front may be considered the design environment. This includes both organizational[20] and computational[21–23] frameworks that allow automation of multidisciplinary analyses. A second front for RLV multidisciplinary design research is the MDO problem formulation. A review of MDO problem formulations and implementation issues is given by Alexandrov and Kodiyalam.[24] In addition to the design environment and the MDO formulation, a third front for MDO research includes approximation modeling. These models are useful in allowing tradeoffs between analysis fidelity and computational complexity at the early stages of design. This concept can also be applied to a single MDO. For example, in approximation/model management optimization,[25] a trust region approach is used to approximate a system objective with a low-fidelity model, update the model at each optimization iteration, and resort to higher-fidelity approximations when needed. Various methods are available to build these initial, low-fidelity models, including response surface models, Taylor series approximations, splines, and Kriging models. In particular, a D-optimal response surface strategy has been implemented for an RLV sizing application using three disciplines: geometry, weights, and aerodynamics.[16] This response surface formulation provides the baseline for the probabilistic optimization approach presented in this paper.

A final area of concern for RLV design research is the optimization objective. As stated earlier, program goals have been expressed in terms of cost objectives, for example, \$1000/lb payload, and risk objectives, for example, 1/10,000 risk of crew loss. It is logical, then, that the design optimization should incorporate these goals. These goals could be incorporated through either the optimization objective function or the constraints. In RLV design, minimizing other parameters considered roughly proportional to cost often approximates cost optimality. Braun and Moore[18] compare a collaborative optimization analysis using four different optimization objectives: development cost, gross liftoff weight, vehicle empty weight, and ΔV (velocity change from the rocket equation).

Incorporating risk goals explicitly in the optimization is a concept that needs significant development in multidisciplinary RLV design. Risk is a concept that is difficult to measure and proves challenging to model. A traditional approach is to model risk via factors of safety. Factors of safety provide a qualitative measure of risk, but can not be translated to probabilistic metrics (such as 1/10,000 risk of crew loss). Another tactic is to model risk from empirical data obtained through testing or historical records. For example, NASA has developed a reliability and maintainability analysis and estimation tool (RMAT), which models RLV operations and supports reliability through a comparison to historical database records from current operational aircraft.[19] Response surfaces are generated from RMAT for use in the optimization of performance reliability. Unfortunately, historical records have limited use for novel designs, and testing is prohibitively expensive for complex systems.

An alternate approach is to estimate risk through simulation of physics-based models by explicitly considering the uncertainty in the input parameters or in the model itself. Deterministic approaches that have been the focus of RLV design optimization methods thus far fail to account for these uncertainties. Therefore, a probabilistic approach is needed for risk-based optimization under uncertainty and is pursued in this paper.

Probabilistic Analysis and Optimization

RLV design optimization to date has been based on a deterministic approach. Input variables are assumed to be nonvarying and the system is assumed to behave exactly as an analysis model predicts. In this case, the analysis output will be deterministic, and there will not be any uncertainty-based metric for assessing risk. A probabilistic approach, on the other hand, allows for random variation in the input variables and can also consider the error between model predictions and true system behavior. In this case, the output will also have random variation. This random variation is characterized by a probability distribution function defined by its shape and a set of distribution parameters, for example, mean and standard deviation. Risk objectives can then be defined in terms of this output uncertainty.[5] A probabilistic optimization will then characterize uncertain objectives and constraints in terms of probability distribution parameters and statistics, for example, minimize μ_Z subject to $P(x_1 < x < x_2) \le p_f$, where μ_z is the mean of output z and p_f is some acceptable probability of failure for x to be in the interval $[x_1, x_2]$.

In the physics-based limit-state method for reliability modeling, a performance function g_i is defined in terms of the random variables corresponding to a failure criterion. Typically $g_i < 0$ represents failure, $g_i > 0$ represents success, and $g_i = 0$ is referred to as the limit state.[5] The probabilities of failure may be evaluated with a number of probabilistic techniques, including simulation methods (for example, Monte Carlo, adaptive importance sampling, Latin hypercube sampling, etc.) or analytical approximation methods [first-order reliability method (FORM), second-order reliability method, first-order second-moment methods].[5] For optimization problems, an analytical approximation method is preferred due to computational efficiency.

Probabilistic optimization has been the focus of several recent research efforts. Optimization formulations have three components (design variables, the objective function, and constraints) leaving a few alternatives for stating the probabilistic problem. First, input variables (including design variables) are uncertain, but can be characterized by their distribution parameters. Thus, optimization problems may have design variables that include mean values, standard deviations, a combination of both, or other parameters describing their randomness.[26] (In addition to the design variables, other input variables may also be modeled as random variables. However, this does not complicate the optimization process because all random variables are considered together in the evaluation of the probabilistic constraint.) Second, the objective function may be in terms of failure probability (for example, minimize probability of failure), an independent cost or performance measure (for example, minimize mean development cost), or may be a cost or performance measure that depends on reliability (for example, minimize total cost = development cost + failure cost × probability of failure). Finally, constraints may include either cost or reliability design goals that are not considered in the objective function.

Another consideration for the probabilistic optimization formulation addresses the level of the failure. Physics-based limit states usually represent component-level events, where probabilities of failure can be calculated fairly easily. System-level failure results from component failures in series, parallel, or a combination of both. Event sequence diagrams may be used to define the system. For large systems with nonindependent components, calculation of system failure probabilities can be time consuming. The branch and bound method has been used to streamline the system calculation,[4] but it is still difficult to employ within an optimization. Optimum design of framed structures has been undertaken, using component-level reliability constraints and a system-level objective function (weight of system structure).[11,15] Oakley et al.[27] combine stochastic optimization with adaptive response surfaces. This work considers two types of uncertainty (variability of operating conditions and uncertainty in extreme values) under a system of multiple load cases. Leheta and Mansour[28] apply a system reliability optimization formulation to structural design of marine stiffened panels. They employ the FORM to determine component reliability and use an approximation for the reliability of a series system that includes multiple failure mechanisms.

Probabilistic optimization problems, also called reliability-based design optimization, have been solved through a number of techniques. These techniques employ standard linear or nonlinear programming algorithms and analytical reliability analysis methods to solve carefully formulated probabilistic problems. In the reliability index approach (RIA), probabilistic constraints are reformulated in terms of reliability indices. In the performance measure approach (PMA), the constraints are transformed through an inverse reliability analysis. RIA and PMA methods are combined in an adaptive scheme that uses RIA when the probabilistic constraint is active, that is, the design point is on the constraint boundary, and PMA when the constraint is inactive.[27] Putko et al.[29] present a methodology using sensitivity derivatives for design optimization using computational fluid dynamics (CFD) codes. Royset et al.[30] present a decoupling approach for three types of probabilistic optimization problems: In this methodology, constraints originally given in terms of reliability indices are replaced by a function representing the limit state minimum within a hypersphere of specified radius.

In the application presented in this paper, a probabilistic formulation is chosen that uses mean values as the design variables, mean dry weight as the objective function, and component failure probabilities (in this case, probability of exceeding a limiting pitching moment value) as constraints. A direct (coupled) approach using FORM is chosen for the reliability analysis. FORM is an analytical approximation method. It is an iterative approach that converges to find the minimum distance β (the reliability index) from the origin to the limit state in the space of equivalent uncorrelated standard normal variables. The probability of failure P_f is approximated as $\Phi(-\beta)$, where Φ is the cumulative distribution function (CDF) of the standard normal distribution. FORM is discussed in more detail hereafter.[5] A generalized reduced gradient algorithm is used for the optimization.

Launch Vehicle Conceptual Design: Deterministic Approach

As a first effort in the RLV multidisciplinary design analysis, low-fidelity second-order response surface models have been developed for a sizing analysis of a wing–body, single stage-to-orbit vehicle.[16] For this application, a launch vehicle is sized to deliver 25,000 lb in payload from the NASA Kennedy Space Center to the International Space Station. The selected vehicle geometry (shown in Fig. 1) has a slender, round fuselage and a clipped delta wing. Elevons provide aerodynamic and pitch control. Vertical tip fins provide directional control and body flaps provide additional pitch control.

Table 1 Design variables

Design variable	Lower bound	Upper bound
Fuselage finess ratio r_f	4	7
Wing area ratio a_w	10	20
Tip-fin area ratio a_{tf}	0.5	3
Body-flap area ratio a_{bf}	0	0
Ballast weight fraction b_l	0	0.04
Mass ratio r_m	7.75	8.25

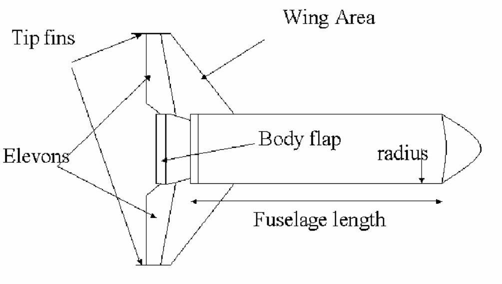

Fig. 1 Second-generation RLV concept.

As a first step in the conceptual design, two disciplines (weights/sizing and aerodynamics) are considered in a constrained optimization problem. A vehicle geometry that minimizes mean dry weight is expected to minimize overall cost, so this is chosen as the objective function. For stability, the pitching moment C_m for the vehicle should be zero or extremely close to zero. In addition, C_m should decrease as the angle of attack increases. This is achieved by adjusting the control surfaces' trim of the vehicle as the angle of attack is increased. Thus, the aerodynamic analysis for pitching moment constrains the optimization.

The optimal vehicle design is determined by six design variables: fineness ratio (fuselage length/radius), wing-area ratio (wing area/radius^2), tip-fin area ratio (tip-fin area/radius^2), body-flap area ratio (body-flap area/radius^2), ballast weight fraction (ballast weight/vehicle weight), and mass ratio (gross liftoff weight/burnout weight). The design variables are summarized in Table 1. For the aerodynamic part of the analysis, three additional variables are required to describe the adjustment of control surfaces to trim the vehicle: angle of attack, elevon deflection, and body-flap deflection. The pitching moment constraint must hold during all flight conditions; nine flight scenarios (constructed with three velocity levels and three angles of attack) are used as a representative sample. The representative velocities (Mach 0.3, 2, and 10) were selected as those originally used in Unal et al.[16] for which response surfaces have already been generated. The control variables used for each of the nine scenarios are given in Table 2. The deterministic optimization problem may then be written as follows: Minimize vehicle dry weight W such that the pitching moment coefficient C_m for each of 9 scenarios is within acceptable bounds $[-0.01, +0.01]$.

This is a multidisciplinary problem requiring the synthesis of information from three analysis codes: a geometry-scaling algorithm, a weights and sizing code (CONSIZ), and an aerodynamic code (APAS). Integrating these codes is somewhat complex because in addition to the variables already described, there are numerous, nondesign variables that are passed between the codes. This effort would be computationally expensive for an optimization algorithm. Thus, Unal et al.[16] conducted two overdetermined D-optimal experimental designs to reduce these analyses to a set of second-order response surface models that relate the vehicle dry weight W to the six geometry variables and the pitching moment coefficient C_m to both the geometry and control variables. (Note: There are 30 independent variables in total. The control variable values are specific to a scenario. All nine scenarios involve adjusting the angle of attack and elevon deflection, but only the supersonic and hypersonic response surface models specifically include body flap deflection as one of the statistically significant random variables.)

In the design of experiments for the weight function, 45 multidisciplinary analyses were conducted according to the design matrix described in Table 3. For each row in the matrix, an analysis is run

Table 2 Control variables

	Nominal angle of attack		Minimum angle of attack		Maximum angle of attack	
Aerocontrol variable	Lower bound	Upper bound	Lower bound	Upper bound	Lower bound	Upper bound
Mach 0.3						
Angle of attack, deg	12	12	5	5	15	15
Elevon deflection, deg	−15	10	−15	10	−15	10
Mach 2.0						
Angle of attack, deg	10	10	5	5	15	15
Elevon deflection, deg	−15	10	−15	10	−15	10
Body flap deflection, deg	−10	10	−10	10	−10	10
Mach 10						
Angle of attack, deg	30	30	25	25	40	40
Elevon deflection, deg	0	30	0	20	0	20
Body flap deflection, deg	0	20	0	20	0	20

Table 3 Six-parameter D-optimal design matrix[2]

Analysis	r_f	a_w	a_{tf}	B_{FL}	b_l	r_m
1	−1	−1	−1	−1	−1	1
2	−1	−1	−1	−1	1	−1
3	−1	−1	−1	1	−1	0
4	−1	−1	−1	1	1	1
5	−1	−1	0	1	−1	−1
6	−1	−1	1	−1	−1	1
⋮	⋮	⋮	⋮	⋮	⋮	⋮
41	1	1	0	0	−1	1
42	1	1	1	−1	−1	−1
43	1	1	1	−1	1	1
44	1	1	1	1	0	−1
45	1	1	1	1	1	1

with design variable values given according to their corresponding column of normalized values. Cells in the matrix with a value of −1 denote the lowest variable value; those with a value of zero denote the midrange value; and those with a value +1 denote the highest variable value. These do not necessarily correspond to the constraint bounds used in the optimization but rather depict the range of values over which the response surfaces are valid. It is important that the optimum domain is within the domain of the response surfaces. If the response surfaces lead to an optimum domain outside the range of the response surfaces, then an adaptive "trust region" strategy may be needed.[31] It is also desirable to check the optimum solution with a full high-fidelity analysis if possible. Also, in the initial conceptual design stage, the feasible response surface ranges may be determined using expert opinion. In this case, the optimization domain is the same as the response surface domain, except that the body-flap area is additionally constrained. Curve fitting the experiment results produces a second-degree polynomial for the dry weight of the vehicle. A similar methodology was used to generate second-degree response surfaces for the pitching moment coefficient. The response surface polynomials are expressed in terms of the normalized variables from the D-optimal matrix (values between −1 and 1), which we will refer to as reduced variables. These are distinguished from the original variables given in Tables 1 and 2.

Once the response surfaces were generated, a gradient-based nonlinear optimizer was used to solve the optimization problem. A verification run of the multidisciplinary analysis was performed at the optimal design point. The result agreed with the response surface prediction within 1%.

Launch Vehicle Conceptual Design: Probabilistic Approach

To reformulate the problem in probabilistic terms, it is restated as follows: Minimize mean weight such that the pitching moment coefficient for all nine scenarios has a low probability (less than 0.1) of failing to be within the acceptable bounds [−0.01, +0.01]. Note here that the output parameters (weight W and pitching moment C_m) are random variables. They cannot be known exactly because the inputs and analysis model, from which they are based, are subject to uncertainty. Therefore, minimizing the mean weight approximates the weight minimization, and the pitching moment constraint is estimated as a probability of failure to be within acceptable bounds. The solution of this revised, probabilistic problem consists of four parts: 1) characterization of random input variables, 2) definition of the limit states for failure, 3) probabilistic analysis, and 4) optimization.

Characterization of Random Input Variables

Original Variables

The first step is to define the uncertainty of the input variables. From the standpoint of the conceptual analysis, these distributions will represent statistical variation in input parameters. However, it is not obvious how this information shall translate into physical phenomena. For fully designed system, these distributions would represent uncertainty between as-built dimensions and that specified by the design. However, details from the conceptual design will inevitably undergo numerous revisions before any kind of physical construction; any relationship between the conceptual design and the as-built condition will be superceded by intermediate higher-fidelity analysis and design. At this stage, enough data are not yet available to characterize the physical uncertainty of the as-built dimensions. However, at this stage, a high level of precision is not required. Therefore, approximate data were constructed based on expert opinion. (The experts were asked to estimate uncertainty of the as-built dimensions based on a full design.) All distributions were assumed normal (a simplifying assumption to facilitate analysis). However, any other distribution can be easily included within the probabilistic framework used here. The mean values μ of the variables are the design variables, and then change during the optimization iterations. The standard deviations σ were assumed to be either one-third of the range or estimated from an assumed coefficient of variation δ where $\sigma = \delta \times \mu$. Table 4 describes the characterization of these original input variables.

Reduced Variables

Because these variables are being computed through linear functions of the original variables, their distribution parameters can be easily found. For example, the original variable for fuselage finess ratio r_f has a range from 4 to 7. The response surfaces use a reduced variable, $\mathrm{FR} = (r_f - 5.5)/1.5$, where 5.5 is the midrange value and 1.5 is the half-range. FR will have a mean $\mu_{\mathrm{FR}} = (\mu_{r_f} - 5.5)/1.5$, and standard deviation $\sigma_{\mathrm{FR}} = \sigma_{r_f}/1.5$. Table 5 describes the reduced variables.

Model Error

In a physics-based reliability model, only a portion of the uncertainty in a system is accounted for through its input parameters. The analytical model for the RLV is a regression model (the response surfaces) of a computational model (the multidisciplinary system analysis) of a conceptual model (based on principles of physics, usually in the form of partial differential equations) of the real system. Regardless of variation in input, the conceptual model does not predict real system behavior exactly, the computational model does not exactly represent the conceptual model, and the regression

Table 4 Statistics of original variables

Design variable	Distribution	Mean	Range	Coefficient of variation	Standard deviation
Geometry variables					
Model error	Normal	0	—	—	0.1
Fuselage finess ratio r_f	Normal	6.2796	—	0.01	0.0628
Wing area ratio a_w	Normal	16.1524	—	0.01	0.1615
Tip-fin area ratio a_{tf}	Normal	0.5	—	0.01	0.005
Body-flap area ratio a_{bf}	Normal	0	—	0.01	0
Ballast weight fraction b_l	Normal	0	—	0.01	0
Mass ratio r_m	Normal	7.75	0.05	—	0.0167
Control variables					
Scenario 1: Mach 0.3, nominal angle of attack					
Angle of attack	Normal	12	0.1	—	0.0333
Elevon deflection	Normal	−7.7336	1	—	0.3333
Scenario 2: Mach 0.3, minimum angle of attack					
Angle of attack	Normal	5	0.1	—	0.0333
Elevon deflection	Normal	−1.3109	1	—	0.3333
Scenario 3: Mach 0.3, maximum angle of attack					
Angle of attack, Mach 0.3 maximum	Normal	15	0.1	—	0.0333
Elevon deflection	Normal	−10	1	—	0.3333
Scenario 4: Mach 2, nominal angle of attack					
Angle of attack	Normal	10	0.25	—	0.0833
Elevon deflection	Normal	−0.3066	1	—	0.3333
Body flap	Normal	−0.3481	1	—	0.3333
Scenario 5: Mach 2, minimum angle of attack					
Angle of attack	Normal	5	0.25	—	0.0833
Elevon deflection	Normal	−5.0628	1	—	0.3333
Body flap	Normal	−5.0156	1	—	0.3333
Scenario 6: Mach 2, maximum angle of attack					
Angle of attack	Normal	15	0.25	—	0.0833
Elevon deflection	Normal	−0.1877	1	—	0.3333
Body flap	Normal	10	1	—	0.3333
Scenario 7: Mach 10, nominal angle of attack					
Angle of attack	Normal	30	0.25	—	0.0833
Elevon deflection	Normal	29.8082	1	—	0.3333
Body flap	Normal	6.4322	1	—	0.3333
Scenario 8: Mach 10, minimum angle of attack					
Angle of attack	Normal	25	0.25	—	0.0833
Elevon deflection	Normal	20	1	—	0.3333
Body flap	Normal	20	1	—	0.3333
Scenario 9: Mach 10, maximum angle of attack					
Angle of attack	Normal	40	0.25	—	0.0833
Elevon deflection	Normal	20	1	—	0.3333
Body flap	Normal	20	1	—	0.3333

model introduces further error. This regression error can be determined from the residuals of the least squares, but it is only one of many sources of error introduced by the model. In addition, the response surfaces were constructed by assuming deterministic values for many input parameters that, in reality, are uncertain. Furthermore, biases are present in the computational model due to system dynamics not captured by the model. Reinelt et al.[32] and Ninness and Goodwin[33] review various strategies for quantifying errors and uncertainty in the errors of computational models. Oberkampf and Trucano[34] also give a thorough review of errors associated with CFD models and their significance in model validation.

Experimental information is not available during the initial stages of design. Also, the fidelity requirements at this state may not warrant sophisticated error modeling. However, in some cases, tolerances on the other input variables may be so tight as to make them effectively deterministic compared to the effect of model error. Thus, it is useful to at least estimate model error in conceptual probabilistic analysis. Several methods for the probabilistic quantification of model error arising from various levels of approximation are currently under development.[35] In this application, the model "error" is considered simply as an additional random variable applied to the predicted pitching moment as a percentage. Here, model error has a mean of 0 and a standard deviation of 10%. Thus, the output pitching moment coefficient, $C_m = C_m(\text{pred}) \times (1 + \text{error})$, where $C_m(\text{pred})$ is the pitching moment predicted from the response surfaces.

Limit States

A limit state defines the boundary between success and failure of the system. In this problem, each of the nine scenarios has two limit states, one for the lower bound and one for the upper bound of C_m (pitching moment coefficient). The lower bound limit state is

$$g_{\text{lower}} = 0.01 + C_m \tag{1}$$

and the upper bound limit state is

$$g_{\text{upper}} = 0.01 - C_m \tag{2}$$

The probability of failure is defined as

$$\begin{aligned} P_f &= P(C_m < -0.01) + P(C_m > 0.01) \\ &= P(g_{\text{lower}} < 0) + P(g_{\text{upper}} < 0) \end{aligned} \tag{3}$$

The probability of failure for each limit state is the volume integral under the joint probability density function of all of the input variables over the failure region, that is, where $g < 0$, as shown in Fig. 2.

FORM

In this method, the minimum distance from the origin to the limit state is expressed as $\beta = \sqrt{[(X'^*)^T(X'^*)]}$, where X'^* is the point of minimum distance from the origin to the limit state. The minimum distance point on the limit state is referred to as the most probable point (MPP). X' is the vector of reduced normal variables. In this case, variables are assumed normal, but they can be transformed into equivalent normal variables for the FORM analysis should a different distribution be appropriate. A linear (first-order) approximation of the volume integral (or failure probability) at the MPP

Table 5 Statistics of reduced variables

Design variable	Mean	Standard deviation
Geometry variables		
Model error, Xe	0	0.1
r_f, X1 (normalized fuselage finess ratio)	0.5198	0.0419
a_w, X2 (normalized wing area ratio)	0.2305	0.0323
a_{tf}, X3 (normalized tip fin area ratio)	−1	0.004
B_{FL}, X4 (normalized body flap area ratio)	−1	0
b_l, X5 (normalized ballast weight fraction)	−1	0
r_m, X6 (normalized mass ratio)	−1	0.6667
Control variables		
Scenario 1: Mach 0.3, nominal angle of attack		
Alpha (derived from angle of attack) −X7	0.9512	0.0159
Delev (derived from elevon deflection) −X8	−0.6130	0.0264
Scenario 2: Mach 0.3, minimum angle of attack		
Alpha (derived from angle of attack) −X7	−2.378	0.0159
Delev (derived from elevon deflection) −X8	−0.1039	0.0264
Scenario 3: Mach 0.3, maximum angle of attack		
Alpha (derived from angle of attack) −X7	2.378	0.0159
Delev (derived from elevon deflection) −X8	−0.7927	0.0264
Scenario 4: Mach 2, nominal angle of attack		
Alpha (derived from angle of attack) −X7	0	0.0396
Delev (derived from elevon deflection) −X8	−0.0243	0.0264
Bflap (derived from body flap deflection) −X9	−0.3481	0.3333
Scenario 5: Mach 2, minimum angle of attack		
Alpha (derived from angle of attack) −X7	−2.378	0.0396
Delev (derived from elevon deflection) −X8	−0.4013	0.0264
Bflap (derived from body flap deflection) −X9	−5.0157	0.3333
Scenario 6: Mach 2, maximum angle of attack		
Alpha (derived from angle of attack) −X7	2.378	0.0396
Delev (derived from elevon deflection) −X8	−0.0149	0.0264
Bflap (derived from body flap deflection) −X9	10	0.3333
Scenario 7: Mach 10, nominal angle of attack		
Alpha (derived from angle of attack) −X7	−0.7927	0.0396
Delev (derived from elevon deflection) −X8	2.3476	0.0264
Bflap (derived from body flap deflection) −X9	6.4322	0.3333
Scenario 8: Mach 10, minimum angle of attack		
Alpha (derived from angle of attack) −X7	−2.378	0.0396
Delev (derived from elevon deflection) −X8	0.7927	0.0264
Bflap (derived from body flap deflection) −X9	20	0.3333
Scenario 9: Mach 10, maximum angle of attack		
Alpha (derived from angle of attack) −X7	2.378	0.0396
Delev (derived from elevon deflection) −X8	0.7927	0.0264
Bflap (derived from body flap deflection) −X9	20	0.3333

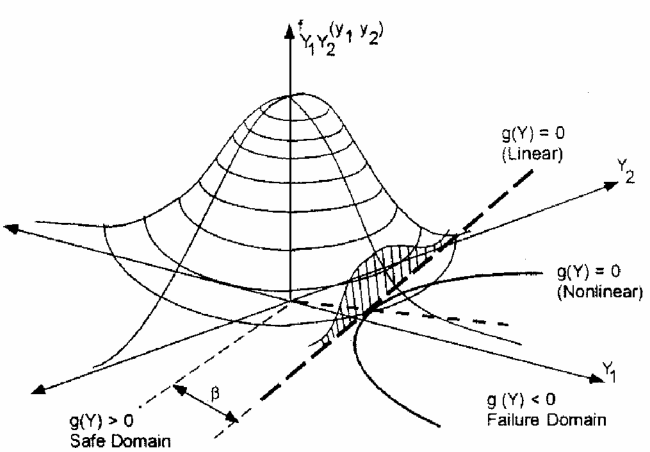

Fig. 2 Limit state and probability of failure.

is computed as $\Phi(-\beta)$, where Φ is the CDF for a standard normal parameter (Fig. 3).

The MPP is found iteratively using the Rackwitz–Fiessler formula (see Ref. 14)

$$X'^{*}_{k+1} = \left(1/\left|\nabla g\left(X'^{*}_{k}\right)\right|^{2}\right)\left[\nabla g\left(X'^{*}_{k}\right)^{t}\left(X'^{*}_{k}\right) - g\left(X'^{*}_{k}\right)\right]\nabla g\left(X'^{*}_{k}\right) \quad (4)$$

Here, X'^{*}_{k+1} is the MPP at the $(k+1)$th iteration, and $\nabla g(X'^{*}_{k})$is the gradient vector (vector of derivatives of the limit state function with respect to each variable). The direction cosines (alphas) at the MPP,

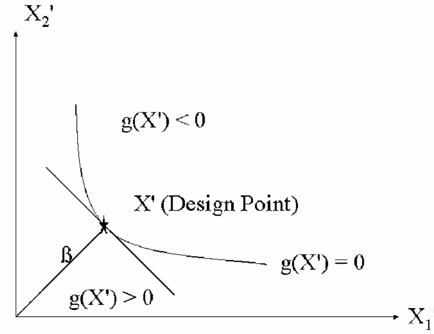

Fig. 3 FORM.

$$\alpha_i = \frac{\partial g}{\partial x_i} \times \sigma_{x_i} \Bigg/ \left|\sqrt{\sum\left(\frac{\partial g}{\partial x_i} \times \sigma_{x^i}\right)^2}\right|$$

are useful byproducts of the FORM method in that they describe the sensitivity of the limit state to each of the input parameters. The vector $\boldsymbol{\alpha}$ is the unit gradient of the limit state g in standard normal space, at the MPP. This information is helpful on several accounts. Variables with low sensitivities can be approximated as deterministic to reduce the computational complexity of the problem. Also, reducing the standard deviation of variables with high sensitivities will achieve the greatest gains in system reliability.

Optimization

As stated earlier, the probabilistic optimization problem is formulated as follows: Minimize mean weight such that the pitching moment coefficient for all nine scenarios has a low probability (less than 0.1) of failing to be within acceptable bounds [−0.01, +0.01]. Optimization is done in the same manner as before, using a gradient-based nonlinear optimizer. However, instead of constraining C_m to be between [−0.01, +0.01], the probability of exceeding the bounds is constrained to be less than some acceptable value. Also, the means of the input variables are the actual design variables that are altered during the optimization, and the mean weight is minimized.

Results and Discussion

Two deterministic and four probabilistic runs are performed, and their resulting optimal dry weights (or mean dry weights) are compared with one another. The deterministic runs were based on factors of safety of 1 and 1.5 and were formulated as follows: Minimize empty weight, subject to $-0.01 \leq C_{m_i}/\mathrm{FS} \leq 0.01$, for $i = 1$–9 scenarios (from Table 5).

After the optimal design was selected deterministically, a FORM probabilistic analysis was performed (assuming random variation of the design variables) to determine the probability that the pitching moment was with the standard bounds [−0.01, 0.01]. The probabilistic runs were based on acceptable probabilities of failure of 5, 10, 15, and 20%. In this case, the following formulation was used: Minimize mean empty weight, subject to $P(-0.01 \leq C_{m_i} \leq 0.01) \leq P_f$.

Figure 4 compares the optimal weight for each analysis. The first deterministic run uses a factor of safety of one, so that C_m was simply constrained to [−0.01, +0.01] as stated in the original deterministic formulation. As would be expected, this method yields the lowest optimal weight. However, such a solution corresponds to a 50% probability that the pitching moment actually fails to be within these bounds. A postoptimization FORM analysis proves this, but it is also evident by inspection. In effect, the deterministic optimization drives the mean of C_m to the boundary.

The second deterministic optimization with a factor of safety of 1.5, in effect, reduces the pitching moment constraint to [−0.667, +0.667]. A postoptimization probabilistic analysis shows that this method gives a 9.75% probability that the true C_m fails to be within the original bounds [−0.01, 0.01]. The probabilistic optimization results show, as expected, that the optimal mean weight is inversely proportional to the required failure probability.

Note that the 1.5 factor of safety compares closely with the 10% failure probability P_f case in both probability of failure (9.75% for

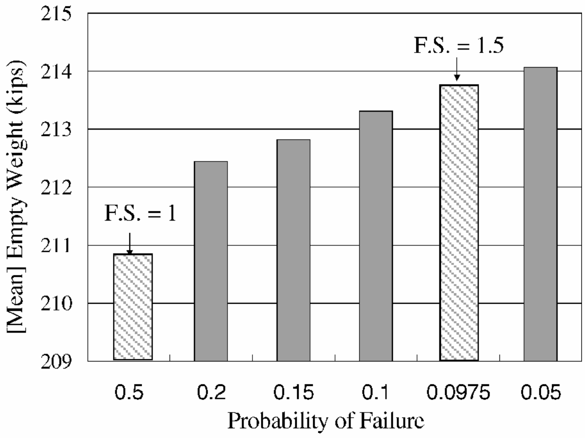

Fig. 4 Weight optimization results.

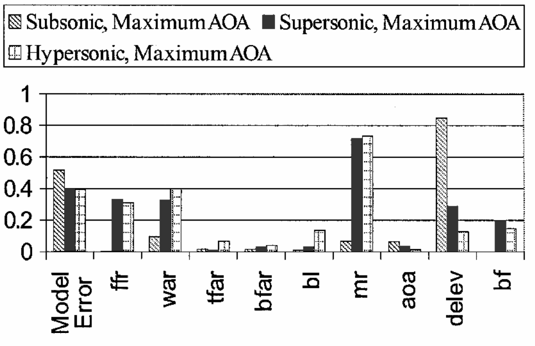

Fig. 5 Variable sensitivities to pitching moment.

the 1.5 FS vs 10% P_f) and optimal mean empty weight [213.7 vs 213.3 kilopounds (kips)]. Although the 1.5 FS approach and the 10% P_f approach both give similar designs, the disadvantage of the factor of safety approach is that it does not quantify the failure probability. Such information is gained only from probabilistic analysis. If we want to improve the probability of satisfying our original constraint by a specific amount, we can not know beforehand what new factor of safety to use. Probabilistic optimization, though it requires more computation than deterministic optimization, is not difficult for simple closed-form analyses that use response surfaces. It enables the designer to consider input variability and in essence, directly design for a reliability requirement.

Figure 5 shows the probabilistic sensitivity indices of the various input variables for three of the nine scenarios: the maximum angle of attack scenarios at each of the three speeds (scenarios 3, 6, and 9 from Table 4). The sensitivity indices are the direction cosines, from the probabilistic analysis

$$\alpha_i = \frac{\partial g}{\partial x_i} \times \sigma_{x_i} \bigg/ \left| \sqrt{\sum \left(\frac{\partial g}{\partial x_i} \times \sigma_{x_i} \right)^2} \right|$$

discussed in an earlier section. They are directly related to the derivatives of the pitching moment failure probability with respect to the input random variables, normalized so that the sum of the squares is one. Note that the probabilistic sensitivity indices combine physical sensitivities (derivatives of the limit state with respect to the design random variables) as well as the scatter (through the σ_{x_i} term) of the random variables. Such information is only available through probabilistic analysis. In addition, the probabilistic sensitivity indices give direct indications for design improvement and optimization. These indices have been used to derive reliability-based design safety factors.[36] Also, these indices help to identify the important variables affecting the system failure probability and, therefore, facilitate decisions with respect to resource allocation for data collection, improved modeling, etc. On the other hand, variables with low-sensitivity indices may be treated as deterministic, thus reducing the computation effort.

It is seen from Fig. 5 that the model error has a significant effect for all scenarios but that the driving effect is mass ratio for the supersonic and hypersonic scenarios and elevon deflection for the subsonic scenario. Similar results are given for other scenarios with the same speeds. (For example, all three subsonic scenarios have high pitching moment sensitivity with respect to elevon deflection.)

Conclusions

This paper has presented and applied a methodology for probabilistic MDO. The combination of response surfaces and first-order reliability analysis provides a valuable tool for system conceptual design. This methodology can be achieved for any defined limit state and could be expanded to incorporate additional probabilistic constraints for more complex problems, for example, for lift and drag failure in this problem. Unlike simulation methods, FORM converges quickly even for very low probabilities of failure and is very conducive to optimization.

The application demonstrated involves codes from three disciplines and considers nine limit states, all related to the pitching moment C_m constraint. In future work, as more disciplines are integrated into the conceptual design process, several different types of constraints may need to be included. Some of the limit states corresponding to these constraints may have a sequential relationship and may be linked through a probabilistic event tree in a system-level analysis. Furthermore, more accurate probabilistic methods are available for use with higher-fidelity codes as design progresses past the initial stage.

Acknowledgments

This research was supported by funds from NASA Langley Research Center (LaRC), Virginia (Cooperative Agreement NCC 1-01031), under the direction of the Multidisciplinary Optimization Branch (Thomas A. Zang). Roger Lepsch from the NASA LaRC Vehicle Analysis Branch provided deterministic optimization data and code as well as valuable technical discussion. In addition, ICASE provided internship support during the summer of 2001. ICASE is operated at NASA LaRC by the Universities Space Research Association under contract with NASA, LaRC. The support is gratefully acknowledged.

References

[1]"2nd Generation RLV System Engineering and Risk Reduction," NASA NRA8-30, Space Transportation Directorate, Marshall Space Flight Center, AL, Oct. 2000.

[2]Karamchandani, A., "Structural System Reliability Analysis Methods," John A. Blume Earthquake Engineering Center, Rept. 83, Stanford Univ., Stanford, CA, 1987.

[3]Swaminathan, S., and Smidts, C., "Event Sequence Diagram Framework for Dynamic Probabilistic Risk Assessment," *Reliability and Engineering System Safety*, Vol. 62, No. 1, 1999, pp. 73–90.

[4]Thoft-Christensen, P., and Murotsu, Y., "The Branch and Bound Method," *Application of Structural Systems Reliability Theory*, Springer-Verlag, Berlin, 1986, pp. 215–267.

[5]Haldar, A., and Mahadevan, S., *Probability, Reliability and Statistical Methods in Engineering Design*, 1st ed., Wiley, New York, 2000, pp. 181–248.

[6]Mahadevan, S., and Dey, A., "Adaptive Monte Carlo Simulation for Time-Dependent Reliability Analysis," *AIAA Journal*, Vol. 35, No. 2, 1997, pp. 321–326.

[7]Mahadevan, S., and Liu, X., "Probabilistic Analysis of Composite Structure Ultimate Strength," *AIAA Journal*, Vol. 40, No. 7, 2002, pp. 1408–1414.

[8]Ryan, R., "Robustness," NASA TP 3363, 1993.

[9]Mahadevan, S., Liu, X., and Xiao, Q., "A Probabilistic Progressive Failure Model of Composite Laminates," *Journal of Reinforced Plastics and Composites*, Vol. 16, No. 11, 1997, pp. 1020–1038.

[10]Cruse, T. A., Mahadevan, S., Huang, Q., and Mehta, S., "Mechanical System Reliability and Risk Assessment," *AIAA Journal*, Vol. 32, No. 11, 1994, pp. 2249–2259.

[11]Frangopol, D. M., "Structural Optimization Using Reliability Concepts," *Journal of Structrual Engineering*, Vol. 111, No. 11, 1985, pp. 2288–2301.

[12]Martz, H. F., and Waller, R. A., *Bayesian Reliability Analysis*, Wiley, New York, 1982.

[13]Mahadevan, S., Zhang, R., and Smith, N., "Bayesian Networks for System Reliability Reassessment," *Structural Safety*, Vol. 23, 2001, pp. 231–251.

[14]Mahadevan, S., and Liu, X., "Probabilistic Optimum Design of Composite Laminates," *Journal of Composite Materials*, Vol. 32, No. 1, 1998, pp. 68–82.

[15]Mahadevan, S., "Probabilistic Optimum Design of Framed Structures," *Computers and Structures*, Vol. 32, No. 3, 1992, pp. 365–374.

[16]Unal, R., Lepsch, R. A., and McMillin, M. L., "Response Surface Model Building and Multidisciplinary Optimization Using D-Optimal Designs," *Proceedings of the Seventh AIAA/USAF/NASA/ISSMO Symposium on Multidisciplinary Analysis and Optimization*, Vol. 1, AIAA, Reston, VA, 1998, pp. 405–411.

[17]Braun, R. D., Powell, R. W., Lepsch, R. A., and Stanley, D. O., "Comparison of Two Multidisciplinary Optimization Strategies for Launch-Vehicle Design," *Journal of Spacecraft and Rockets*, Vol. 32, No. 3, 1995, pp. 404–410.

[18]Braun, R. D., and Moore, A. A., "Use of the Collaborative Optimization Architecture for Launch Vehicle Design," *Proceedings of the Sixth AIAA/USAF/NASA/ISSMO Symposium on Multidisciplinary Analysis and Optimization*, Vol. 1, AIAA, Reston, VA, 1996, pp. 306–318.

[19]Unal, R., Morris, W. D., White, N. H., and Lepsch, R. A., "Modeling and Simulation of Reliability and Maintainability Parameters for Reusable Launch Vehicles Using Design of Experiments," American Society for Engineering Management, Oct. 1998.

[20]Monell, D. W., and Pinland, W. M., "Aerospace Systems Design in NASA's Collaborative Engineering Environment," *Acta Astronautica*, Vol. 47, Nos. 2–9, 2000, pp. 255–264.

[21]Salas, A. O., and Townsend, J. C., "Framework Requirements for Multidisciplinary Optimization Application Development," *Proceedings of the Seventh AIAA/USAF/NASA/ISSMO Symposium on Multidisciplinary Analysis and Optimization*, Vol. 1, AIAA, Reston, VA, 1998, pp. 261–271.

[22]Padula, S. L., Korte, J. J., Dunn, H. J., and Salas, A. O., "Multidisciplinary Optimization Branch Experience Using iSight Software," NASA TM 1999-209714, Nov. 1999.

[23]"Environment for Launch Vehicle Integrated Synthesis (ELVIS)," TA 725-10-11-05, NASA Langley Research Center, Collier Research, Inc., Genes Systems LLC, and Raytheon Corp., Sept. 2001.

[24]Alexandrov, N. M., and Kodiyalam, S., "Initial Results of an MDO Method Evaluation Study," *Proceedings of the Seventh AIAA/USAF/NASA/ISSMO Symposium on Multidisciplinary Analysis and Optimization*, Vol. 2, AIAA, Reston, VA, 1998, pp. 1315–1327.

[25]Alexandrov, N. M., and Lewis, R. M., "First-Order Frameworks for Managing Models in Engineering Optimization," 1st International Workshop on Surrogate Modeling and Space Mapping for Engineering Optimization, Nov. 2000.

[26]Kowal, M., and Mahadevan, S., "Uncertainty-Based Multi-Disciplinary Optimization," AIAA Paper 98-4915, Sept. 1998.

[27]Oakley, D. R., Sues, R. H., and Rhodes, G. S., "Performance Optimization of Multidisciplinary Mechanical Systems Subject to Uncertainties," *Probabilistic Engineering Mechanics*, Vol. 13, No. 1, 1998, pp. 15–26.

[28]Leheta, H. W., and Mansour, A. E., "Reliability-Based Method for Optimal Structural Design of Stiffened Panels," *Marine Structures*, Vol. 10, No. 5, 1997, pp. 323–352.

[29]Putko, M. M., Newman, P. A., Taylor, A. C., and Green, L. L., "Approach for Uncertainty Propagation and Robust Design in CFD Using Sensitivity Derivatives," AIAA Paper 2001-2528, June 2001.

[30]Royset, J. O., Der Kiureghian, A., and Polak, E., "Reliability-Based Optimal Structural Design by the Decoupling Approach," *Reliability Engineering and System Safety*, Vol. 73, No. 3, 2001, pp. 213–221.

[31]Zou, T., Mahadevan, S., Mourelatos, Z., and Meernik, P., "Reliability Analysis of Automotive Body–Door Subsystem," *Reliability Engineering and System Safety*, Vol. 78, 2002, pp. 315–324.

[32]Reinelt, W., Garulli, A., and Ljung, L., "Comparing Different Approaches to Model Error Modeling in Robust Identification," *Automatica*, Vol. 38, 2002, pp. 787–803.

[33]Ninness, B., and Goodwin, G., "Estimation of Model Quality," Centre for Industrial Control Science and Dept. of Electrical and Computer Engineering, TR EE9437, Univ. of Newcastle, Callaghan, New South Wales, Australia, 1994.

[34]Oberkampf, W. L., and Trucano, T. G., "Verification and Validation in Computational Fluid Dynamics," Sandia National Labs., SAND2002-0529, Albuquerque, NM, March 2002.

[35]Rebba, R., "Computational Model Validation Under Uncertainty," M.S. Thesis, Dept. of Civil and Environmental Engineering, Vanderbilt Univ., Nashville, TN, Dec. 2002.

[36]Ang, A. H.-S., and Tang, W. H., *Probability Concepts in Engineering Design, Vol. II, Decision, Risk and Reliability*. Wiley, New York, 1984, pp. 340–346.

J. A. Martin
Associate Editor